Bulletin of the Seismological Society of America, Vol. 86, No. 1A, pp. 19–31, February 1996

Simultaneous Inversion for Earthquake Location and Velocity Structure Beneath Central Costa Rica

by Marino Protti, Susan Y. Schwartz, and George Zandt*

Abstract We have imaged the complex crustal and upper mantle structure beneath central Costa Rica using *P*-wave arrival times from locally recorded earthquakes. Thurber's (1983) iterative inversion method is used to simultaneously estimate velocities along a three-dimensional grid and hypocentral parameters of local earthquakes. Our data consist of over 12,000 arrival times from more than 1300 earthquakes recorded by stations of a permanent seismographic network in Costa Rica. Our resulting velocity model correlates well with mapped geologic units at very shallow depth and with tectonic features at greater depth. We find low velocities (4.0 to 4.8 km/sec) in the shallow crust (above 10 km) near the active volcanoes and associated with a NW–SE trending late Cretaceous to late Tertiary sedimentary basin southeast of Herradura peninsula. High velocities (5.4 to 5.7 km/sec) in the shallow crust correlate with outcrops of late Jurassic to early Tertiary ultramafic ophiolitic units and with basic Tertiary volcanic units. At depths between 20 and 30 km, high velocities (6.8 to 7.2 km/sec) are associated with the subducting Cocos plate under Costa Rica and two prominent low-velocity bodies (6.3 to 6.5 km/sec) are present about 30 km trenchward of the volcanic arc and along the projection of the aseismic Cocos Ridge as it subducts beneath Costa Rica. The thickened oceanic crust of the Cocos Ridge is most likely responsible for its low velocities. The deep low-velocity anomaly located trenchward of the axis of the volcanoes may indicate the presence of a low-density intrusive resulting from an earlier phase of magmatism, possibly the late Miocene episode that produced the Talamanca intrusive complex.

Introduction

The subduction of the Cocos plate under Central America, on the western margin of the Caribbean plate, is the main process controlling Tertiary and Quaternary tectonic activity in the region. Costa Rica is located at the southern terminus of this collision zone (Fig. 1), where the interaction of these plates with the Nazca plate and with the Panama block creates a complicated tectonic setting.

Subduction of the Cocos plate under Costa Rica occurs at rates from 86 to 95 mm/yr from northern to southern Costa Rica, respectively (computed from DeMets *et al.*, 1990). As a consequence of this subduction process, an active volcanic chain runs from Guatemala to central Costa Rica. Remnants of late Tertiary volcanism of basic composition are widely exposed trenchward from this arc in northern and central Costa Rica and mainly toward the back-arc in the south (Fig. 2). Along the western margin of Costa Rica, this subduction process has also uplifted and exposed ultramafic ophiolitic units of late Jurassic to early Tertiary age (Fig. 2). In southern Costa Rica, the shallow subduction of young oceanic lithosphere (Protti *et al.*, 1994) hinders active volcanism and a batholith of intermediate composition (the Talamanca Cordillera) constitutes the inner arc. The Talamanca Cordillera lies on the Panama block. The western boundary of the Panama block with the Caribbean plate is a wide fan-shaped transcurrent shear zone that runs from the Caribbean sea to the Pacific ocean, across central Costa Rica (Fig. 1). Suggestions and evidence in favor of the existence of this developing plate boundary have been given by Ponce and Case (1987), Jacob and Pacheco (1991), Güendel and Pacheco (1992), Goes *et al.* (1993), Fan *et al.* (1993), Fisher *et al.* (1994), and Protti and Schwartz (1994). Incipient subduction of the Caribbean plate under the northern margin of the Panama block seems to be ongoing along the north Panama deformed belt (Silver *et al.*, 1990), where the 1991, Valle de la Estrella earthquake occurred (Goes *et al.*, 1993; Fan *et al.*, 1993; Protti and Schwartz, 1994). It can be expected from this tectonic setting that a complex crustal and upper mantle structure exists under Costa Rica.

*Present address: Department of Geosciences, University of Arizona, Tucson, Arizona 85721.

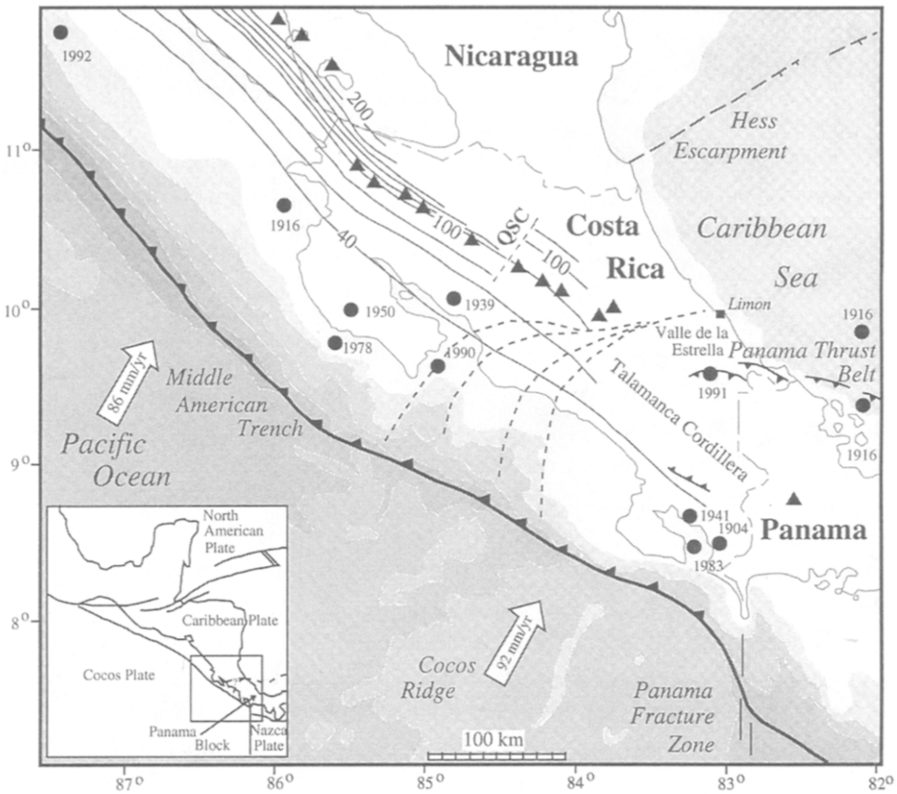

Figure 1. Tectonic setting of southern Central America and geometry of the top of the Wadati-Benioff zone (solid contours) from Protti *et al.* (1994). Filled circles indicate the location of large ($M_S \geq 7.0$) earthquakes of this century. Triangles are active volcanoes. Convergence velocities between Cocos and Caribbean plates were computed from DeMets *et al.* (1990). QSC: Quesada sharp contortion. Inset: major plate boundaries in Central America and location of larger-scale map. Dashed lines across central Costa Rica schematically represent the shear zone that marks the boundary between the Caribbean plate and the Panama block.

The multiplate interaction in Costa Rica explains the higher seismic activity of this country with respect to the rest of Central America, with seismic sources of different genesis and depths. Events less than 30-km deep occur (a) associated with the subduction of the Cocos plate under the Caribbean plate and Panama block; (b) along the Panama fracture zone, the plate boundary between the Cocos and Nazca plates (Fig. 1); (c) as interplate activity between the Caribbean plate and the Panama block; (d) as intraplate deformation of these tectonic units; and (e) associated with the active volcanic arc. Intermediate-depth earthquakes (down to 200 km) occur as internal deformation of the subducted Cocos plate.

Since 1984, the Costa Rica Volcanological and Seismological Observatory of the National University (OVSICORI-UNA) has been operating a permanent short-period seismic network with countrywide coverage (Güendel *et al.*, 1989), jointly with the Charles F. Richter Seismological Laboratory of the University of California at Santa Cruz. Figure 3 shows the spatial distribution of stations of this permanent network as well as temporary stations deployed for aftershock monitoring and study of specific regions. Between April 1984 and December 1991, this network located over 13,000 events, including the two most recent large earthquakes in Costa Rica: the 25 March 1990 (M_w 7.0) and the 22 April 1991 (M_w 7.7) earthquakes (Fig. 1) and their aftershock sequences. The permanent network has its smallest station separation in central Costa Rica where nearly 70% of the country's population lives. It is from this region that most of the seismic activity has been recorded, making it the most suitable region for joint velocity and hypocenter determination.

Imaging the complex structure beneath central Costa Rica is the goal of this work. Knowledge of crustal thickness and regionally appropriate velocities will improve the routine determination of earthquake locations and focal mechanisms and help in understanding the processes producing large earthquakes on both sides of Costa Rica. Additionally, three-dimensional images of the velocity structure of the crust and upper mantle underlying the volcanic chain will help address fundamental questions about magmatic processes.

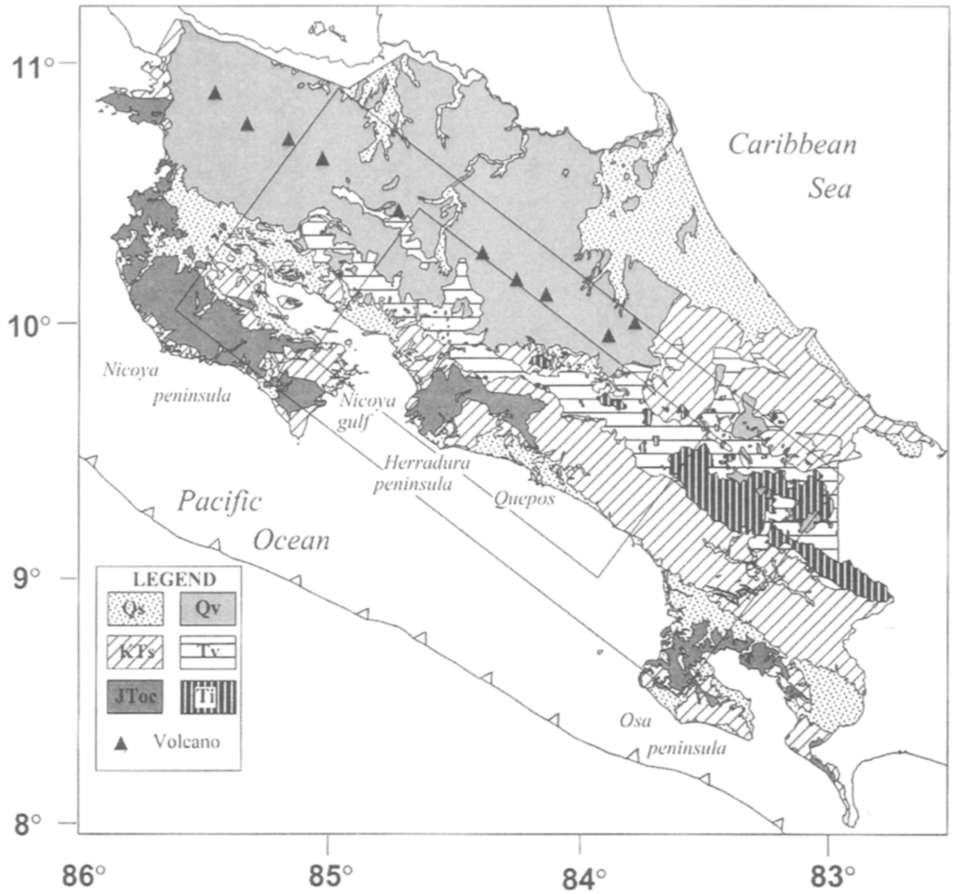

Figure 2. Geologic map of Costa Rica modified after Ludington *et al.* (1987): JToc: oceanic crustal rocks (Late Jurassic to Early Tertiary); KTs: sedimentary rocks (Late Cretaceous to Late Tertiary); Ti: intrusive rocks (Tertiary); Tv: volcanic rocks (Tertiary); Qv: volcanic rocks (Quaternary); Qs: sedimentary rocks (Quaternary). Boxes indicate areas investigated in this work.

Previous Work on Velocity Structure beneath Costa Rica

The *P*-wave velocity structure in northern Costa Rica has been previously studied by Matumoto *et al.* (1977) and by Liaw (1981). Matumoto *et al.* (1977) reported a three-layer crust with velocities of 5.1, 6.2, and 6.6 km/sec, with thicknesses of 8.2, 12.9, and 22.3 km, respectively, overlying a 7.9 km/sec upper mantle. Liaw (1981) simultaneously inverted travel times from 50 local earthquakes for hypocentral and velocity parameters. He obtained a three-layer upper crust with velocities of 5.04, 5.88, and 5.94 km/sec, with thicknesses of 5.2, 2.0, and 13.9 km, respectively, overlying a 6.42 km/sec lower crust.

These models comprise the primary velocity information available for Costa Rica but are inadequate for most regions of the country since the complex tectonic setting suggests a heterogeneous structure throughout the country. The deep Moho (43.4 km) obtained by Matumoto *et al.* (1977) is difficult to reconcile with the thin (20 to 30 km) crust generally associated with active plate margins. The inadequacy of existing velocity models to accurately represent the structure beneath large regions of Costa Rica motivated us to undertake determination of a three-dimensional velocity structure.

Method

We used the iterative linearized inversion technique of Thurber (1983), which incorporates the parameter separation method of Pavlis and Booker (1980) to simultaneously estimate velocities along a three-dimensional grid and hypocentral parameters of locally recorded earthquakes. The computer code we utilized was originally written by Thurber (1983) and modified by Eberhart-Phillips (1986, 1990). Travel times are calculated using the approximate raytracing algorithm (ART) of Thurber (1983), where the path with the least travel time is selected from a suite of circular arcs connecting the hypocenter with the stations. An iterative pseudobending approach is then applied to the selected arc to better approximate the true ray path in accord with the local velocity gradient, by perturbing the ray path using a geometric interpretation of the ray equation (Um and Thurber, 1987). The velocity structure in the model volume is parameterized by assigning velocity values at the intersections (grid points) of a three-dimensional mesh. Velocities and partial derivatives at any particular location on the ray path in this volume are computed by linear interpolation among the surrounding eight grid points. This results in gradational changes in velocity through the volume rather than sharp velocity discontinuities. All earthquakes are first located in an initial velocity structure. Perturbations to velocities and hypocentral parameters are determined by solving the matrix equation $\mathbf{t} = \mathbf{Mm}$ using damped least-squares, where $\mathbf{m}$ and $\mathbf{t}$ are vectors of model perturbations and arrival-time residuals, respectively, and $\mathbf{M}$ is the matrix of hypocentral and velocity partial derivatives. The inversion is performed iteratively until no statistically significant improvement to the model is achieved.

The model resolution R is computed for the final iteration and is given by

$$R = (\mathbf{M}^T\mathbf{M} + \mathbf{L})^{-1}\,\mathbf{M}^T\mathbf{M}, \tag{1}$$

where $\mathbf{L} = \mathbf{I}\phi^2$ ($\mathbf{I}$ is the identity matrix and ϕ^2 is the damping parameter) is the matrix of damping parameters. In general, if the resolution matrix is equal to the identity matrix, each model parameter is uniquely determined, and the model has perfect resolution. In real applications, this rarely happens; in the best cases, the diagonal elements of the resolution matrix have values close to one and the values of the off-diagonal elements decrease rapidly and symmetrically to zero away from the diagonal elements. In velocity inversions, low values of the diagonal elements at a particular node indicate poor ray coverage of that node; high off-diagonal values indicate that the inverted velocity is influenced by anomalies away from that node and may also be the result of uneven sampling of the volume surrounding the node. For a nonlinear inversion, R describes the resolution of a linear problem that is close to the nonlinear one and therefore approximates model resolution. Although not exact, evaluation of R in our case is still very useful for assessing model resolution.

Application to Central Costa Rica

Data

In our inversions, we used arrival times from local earthquakes recorded at 46 short-period, vertical-component stations during the period from 1984 to 1991. Twenty-five of the stations are part of OVSICORI's permanent seismographic network; the rest of the stations were part of temporary arrays deployed for specific studies and for aftershock and seismic swarm monitoring. Figure 3 is a map of the spatial distribution of stations of these networks; station symbols indicate the number of arrivals we used from each station.

We selected 1352 events from a suite of over 13,000 earthquakes (Fig. 4) for inclusion in the inversion. Selection of the events was made to maximize ray coverage and reduce redundancy, particularly from aftershock zones and seismic

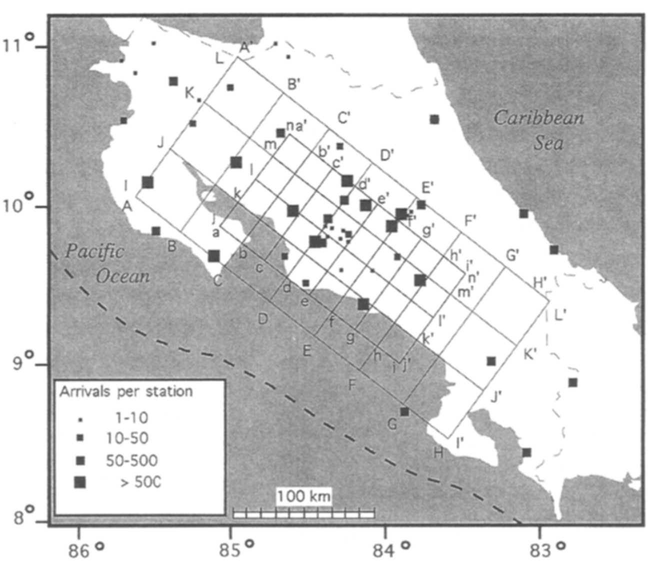

Figure 3. Location of coarse (40 × 40 × 10 km) and fine (20 × 20 × 10 km) grids for velocity determination and location of seismic stations classified by number of arrivals at each station.

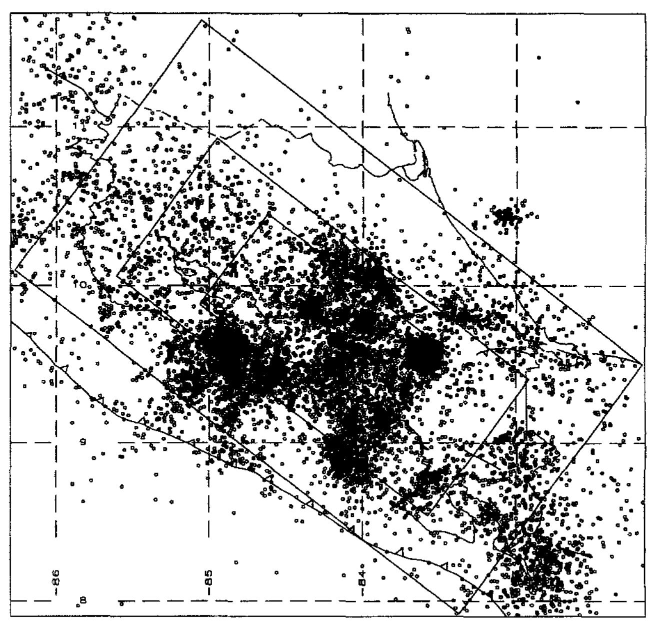

Figure 4. Seismicity recorded by the local network (OVSICORI-UNA) from April 1984 to December 1991. 1352 of these earthquakes (located within the outermost box) were used in our inversions.

swarm areas. Given the uneven distribution of earthquakes, selection criteria were different for different areas. About 65% of the events have focal depths shallower than 30 km and 70% have eight or more arrival times. We included events outside of the velocity grid (Fig. 4) to improve coverage of outer nodes. We used only *P*-wave arrival times since the seismic network is mainly composed of vertical-component stations and *S*-wave arrival times are difficult to determine. Horizontal-component recordings are generally necessary for accurate *S*-wave arrival-time picks. A total of 12,746 arrival measurements were used in our inversions.

Procedure

All events in the data base were initially relocated using the program HYPOINVERSE (Klein, 1978) and the one-dimensional *P*-wave velocity structure shown in Figure 5. In the upper crust, this velocity model corresponds to that proposed by Matumoto *et al.* (1977) for northern Costa Rica, while in the lower crust and upper mantle, it corresponds to that obtained by Zhao *et al.* (1992), for northern Honshu, Japan, a region tectonically similar to Costa Rica.

We inverted arrival-time residuals for velocities at two different scales: first, on a grid of 280 × 120 × 50 km with a spacing of 40 km horizontally and 10 km vertically, and then on a smaller grid with a volume of 160 × 80 × 50 km^3 having a horizontal spacing of 20 km and the same vertical spacing of 10 km (Fig. 3). As a starting model for the inversions performed on the large grid, we used velocities linearly increasing with depth similar to the flat velocity model used in the HYPOINVERSE relocations (Fig. 5). Even though this is a simple model for a region with expected strong-velocity contrasts, it ensures that the final velocity anomalies we obtain are those required by the data and are not due to peculiarities of the initial model (Eberhart-Phillips, 1990). We did test several other one-dimensional starting models (with nodes less separated in depth to accentuate velocity discontinuities), and in general, these models resulted in a decrease in resolution without substantial differences in the final velocity models. We also tried a two-dimensional starting velocity structure, which included the subducting slab as a high-velocity region, and found that it produced results very similar to those of the one-dimensional initial model. We used results of the large-volume inversions as a starting model for inversions along the fine grid.

Damped least-squares inversions require selection of a damping parameter to suppress the instabilities that result in large model changes that occur for near-zero eigenvalues. We follow the empirical methods proposed by Eberhart-Phillips (1986) and Verdonck and Zandt (1994) to choose an appropriate damping parameter for our inversion. Optimal damping values result in both small perturbations to model parameters, **m**, and low travel time residuals, **t**, after the first iteration as well as high resolution and low standard errors for model parameters after convergence. Figure 6 shows the results of our test runs with different damping values. For our final model, we chose a value of 200 for both

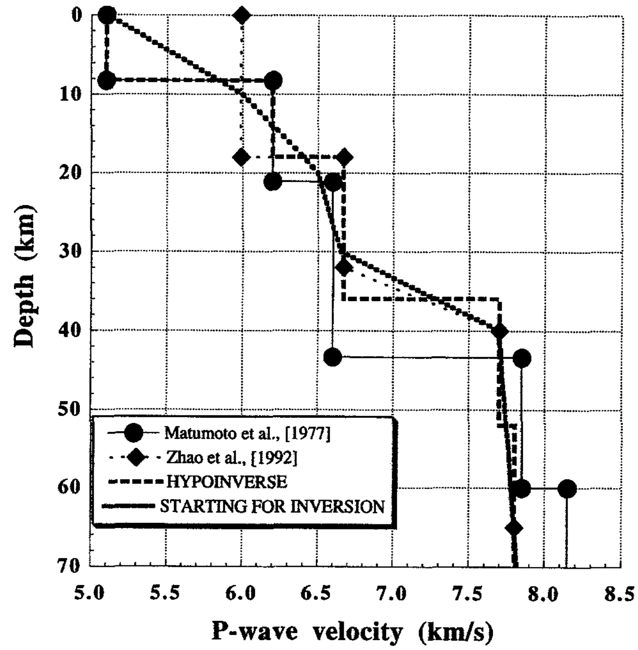

Figure 5. One-dimensional velocity models discussed in this article. Initial travel times were computed after relocating all events with the dashed (HYPOINVERSE) model resulting from the combination of the models proposed by Matumoto *et al.* (1977) for northern Costa Rica and by Zhao *et al.* (1992) for northern Honshu. We started the velocity inversion using the linearly increasing velocity structure (dotted) that follows the velocity model used in the HYPOINVERSE relocations.

the large- and small-volume inversions. This value produced low model ($|\mathbf{m}|^2$) and data ($|\mathbf{t}|^2$) variances after the first iteration and provided a good compromise between relatively high-average resolution and low-average standard error (values averaged for all grid points).

In addition to the weights assigned by seismogram readers at OVSICORI-UNA, arrival times for the inversion were weighted based on hypocentral distance and travel-time residuals. Arrivals with large hypocentral distances and high residuals were given less weight in the inversion. Full weight (1.0) was given to event-station pairs with hypocentral distances less than 75 km and residuals less than 0.5 sec. Weight was linearly decreased to zero for distances and residuals greater than 150 km and 1 sec, respectively.

Results and Discussion

Resolution

The model resolution, computed from equation (1), allows the significance of particular features of the velocity maps to be assessed. The number of rays passing near each grid intersection controls the resolution at that node and arises from the station coverage, earthquake distribution, and

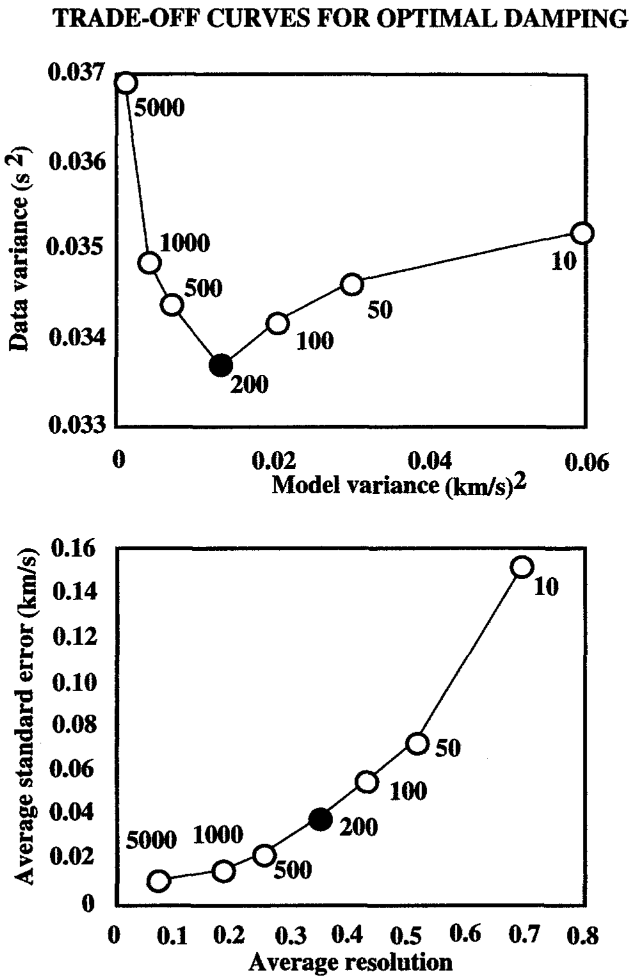

Figure 6. Empirical determination of damping parameter for velocity inversions. Optimal damping values result in both low model and data variance after the first iteration as well as high resolution and low standard error after convergence. We chose a value of 200 for our inversions.

node spacing. Increasing any of these parameters results in an improvement in resolution. We are using the maximum number of stations available in our data base. Increasing the node spacing improves the resolution but smoothes velocity anomalies over a larger volume, making a correlation with tectonic units difficult. Conversely, inverting for small anomalies by reducing the node spacing causes a considerable decrease in resolution. We tried to maintain at least 500 rays passing near most nodes by inverting a large volume with a coarse (40 km) node spacing and a small volume contained within the large volume with a fine (20 km) grid spacing. Decreasing the damping factor will also increase resolution but at the expense of an increased standard error. As described in the previous section, we choose an optimal value of the damping parameter that yields low data variance, low solution variance, and low standard error with a relatively good average resolution (0.35 and 0.32 for the large and small volumes, respectively).

The highest values of the resolution matrix were, in most cases, along the diagonal element, indicating that the velocity at each node is influenced mainly by rays passing near that node (Verdonck and Zandt, 1994). For nodes with diagonal element resolution above the mean, the magnitude of the off-diagonal elements decreased rapidly and symmetrically away from the diagonal. Where the diagonal element is lower than the average, off-diagonal elements were high, indicating vertical smearing for shallow nodes and horizontal smearing for deeper nodes. Vertical smearing may be due to these shallow nodes being influenced by vertical rays from deeper events, while horizontal smearing is attributed to the presence of more horizontal ray paths at depth (Verdonck and Zandt, 1994).

Given the distribution of both seismic stations and earthquake sources, our model resolution varies drastically over the inverted volume. High resolution exists as expected in the central part of the study area where station spacing is the smallest and above 30 km in depth where most of the earthquakes occur (Figs. 7 to 9). This high-resolution zone, with values above 0.5, forms an east–west band along 9.8° N with widths of approximately 80 km at the surface and 100 km at 10 and 20 km in depth (Figs. 7a through 7c). At 30 km in depth and below, good resolution exists only along profile line J-J′ (Figs. 3 and 7d) and below the entrance of the Nicoya Gulf. The small-volume study region is mainly contained within high-resolution regions (Fig. 8).

At shallower depths, we lose resolution toward the north and back-arc as a result of both lower seismic activity and because the few stations in these regions were only installed in 1991. Toward the south, resolution is poor mainly due to large station spacing. We have poor resolution below 30 km in depth, with the exception of regions in and surrounding the subducting slab. This is due to the occurrence of "mantle" earthquakes selectively within the slab.

Crustal Structure beneath Costa Rica

We performed inversions with and without inclusion of station corrections with the major difference in results being a reduction in the magnitude of velocity anomalies at all depths calculated with station delays. While the overall pattern of faster and slower-than-average velocities did not change with the inclusion of station corrections, the perturbation in *P*-wave velocities in the shallowest layer (between 0 and 10 km) reduced from just over 20% to 13%. Differences in percent velocity perturbation of no more than 2% were obtained for the deeper layers. The benefit of using station corrections in the simultaneous inversion for hypocentral and velocity structure parameters is controversial. While some investigators choose to include station corrections (e.g., O'Connell and Johnson, 1991; Verdonck and Zandt, 1994), Thurber (1992) found that for a simple source-receiver geometry, incorporation of station corrections into synthetic tests of earthquake location and velocity structure inversion led to a serious underestimation of lateral velocity heterogeneity. Furthermore, many studies using station cor-

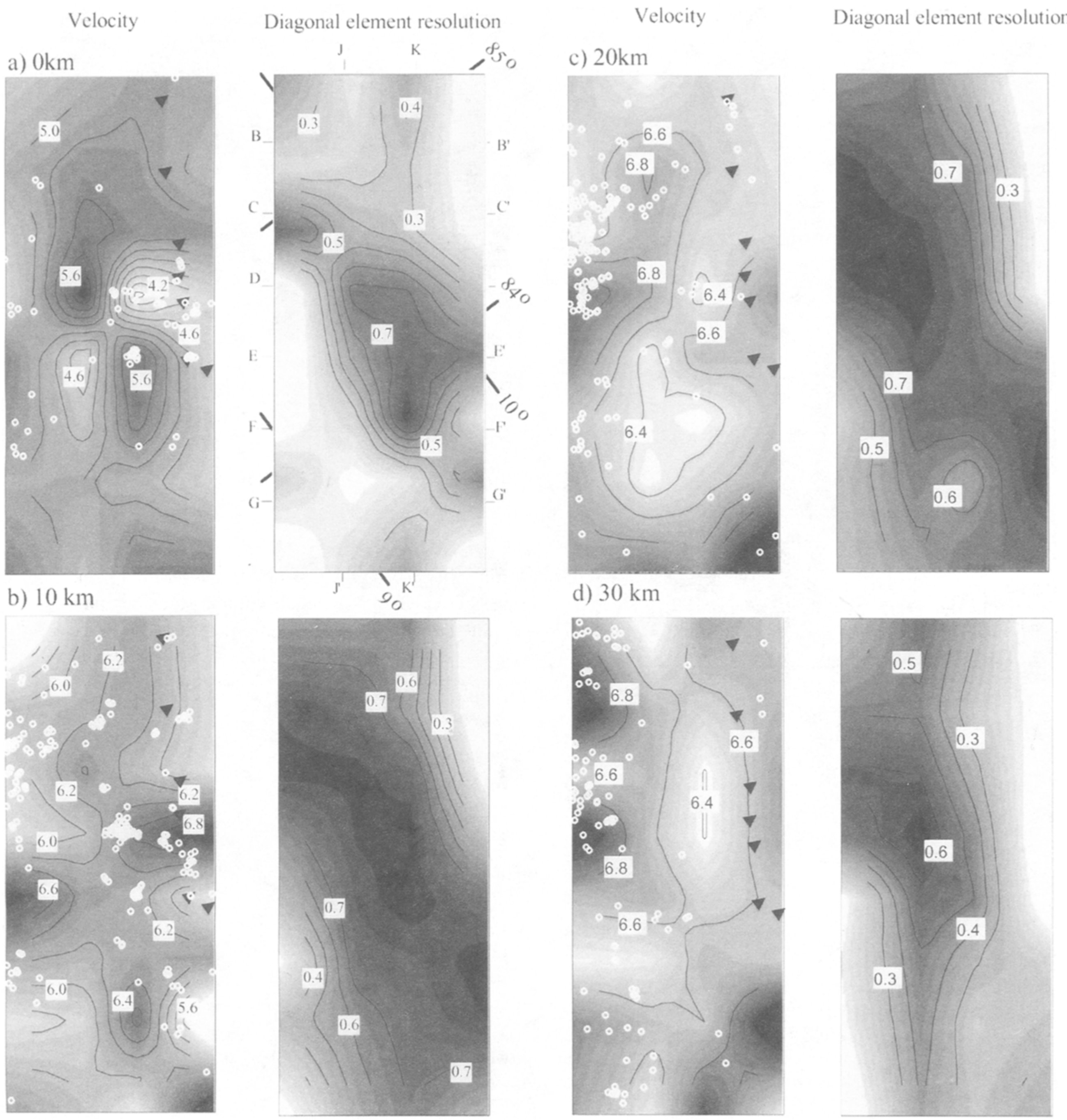

Figure 7. Results of our inversion for *P*-wave velocity (contour interval 0.2 km/sec) and diagonal element resolution (contour interval 0.1) for the coarse (40 × 40 × 10 km) grid and relocated seismicity (white circles). (a) Slice at a depth of 0 km with earthquakes shallower than 5 km; (b) slice at 10 km and earthquakes with focal depth between 5 and 15 km; (c) slice at 20 km and earthquakes with focal depths from 15 to 25 km; (d) slice at 30 km and earthquakes with focal depth from 25 to 35 km. Solid triangles show the location of active volcanoes. Letters correspond to those shown in Figure 3.

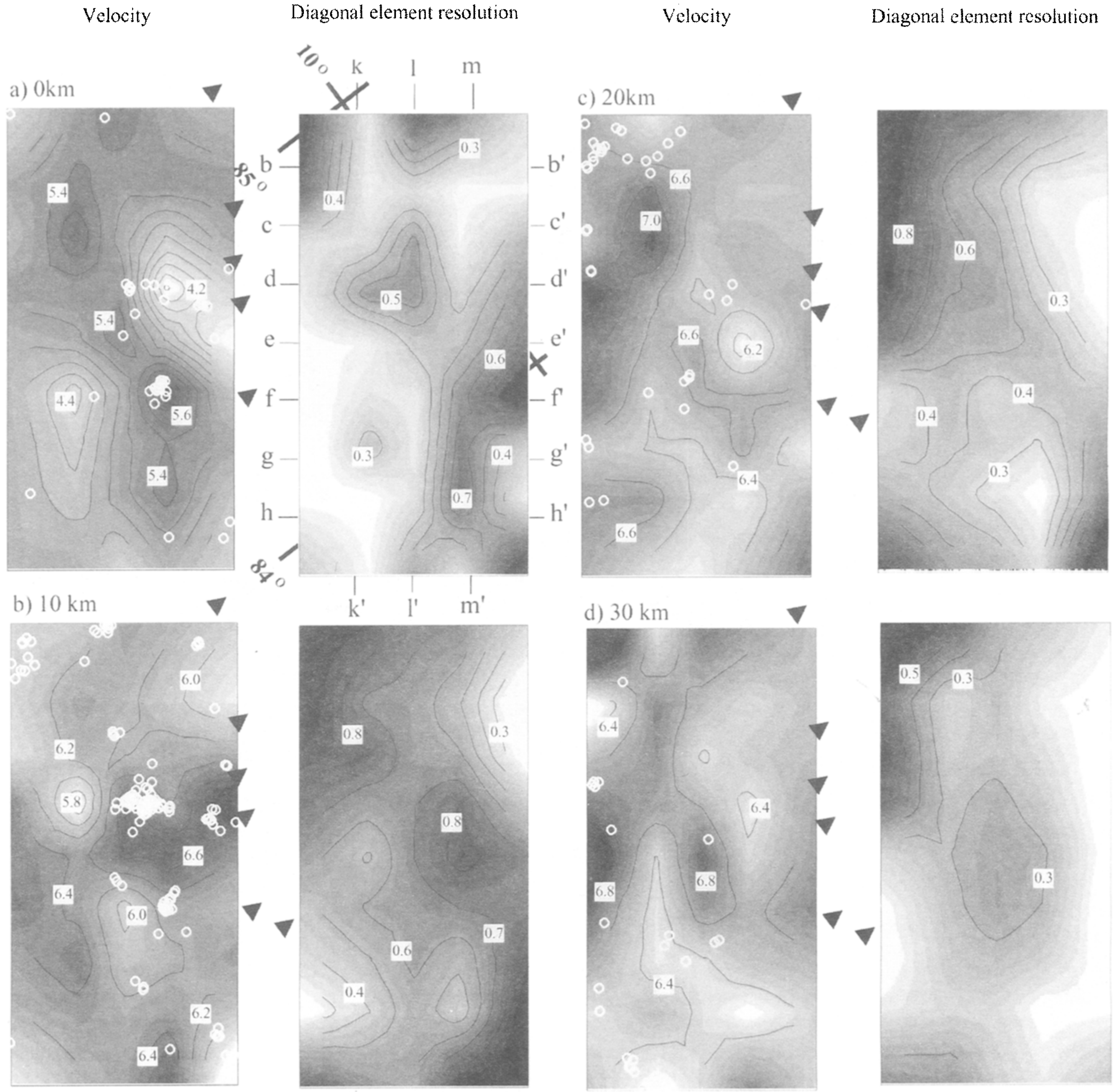

Figure 8. (a) through (d) Results of our inversion for *P*-wave velocity, diagonal element resolution, and relocated seismicity (white circles) for the fine (20 × 20 × 10 km) grid. Conventions are the same as Figure 7.

rections restrict the amount of travel-time residual contributing to station statics by either setting a maximum value that station delays can attain (O'Connell and Johnson, 1991) or by adjusting the station correction damping parameter (Verdonck and Zandt, 1994). Since a significant trade-off between near-surface velocity heterogeneity and station statics exists, the decision to include station corrections in velocity inversions must be made by the investigators depending on their specific situation. In our case, the station corrections computed displayed a regional trend, with groups of nearby stations yielding similar delays. We choose to present results computed without station corrections to avoid isolating what we believe to be regional velocity variations to small regions beneath the stations. While this will undoubtedly distribute a component of the very near-station velocity anomalies throughout a larger volume, we are careful to only interpret the most robust features of our velocity model, specifically those that are common to inversions performed both with and without station corrections.

Near the surface, we can resolve one low-velocity

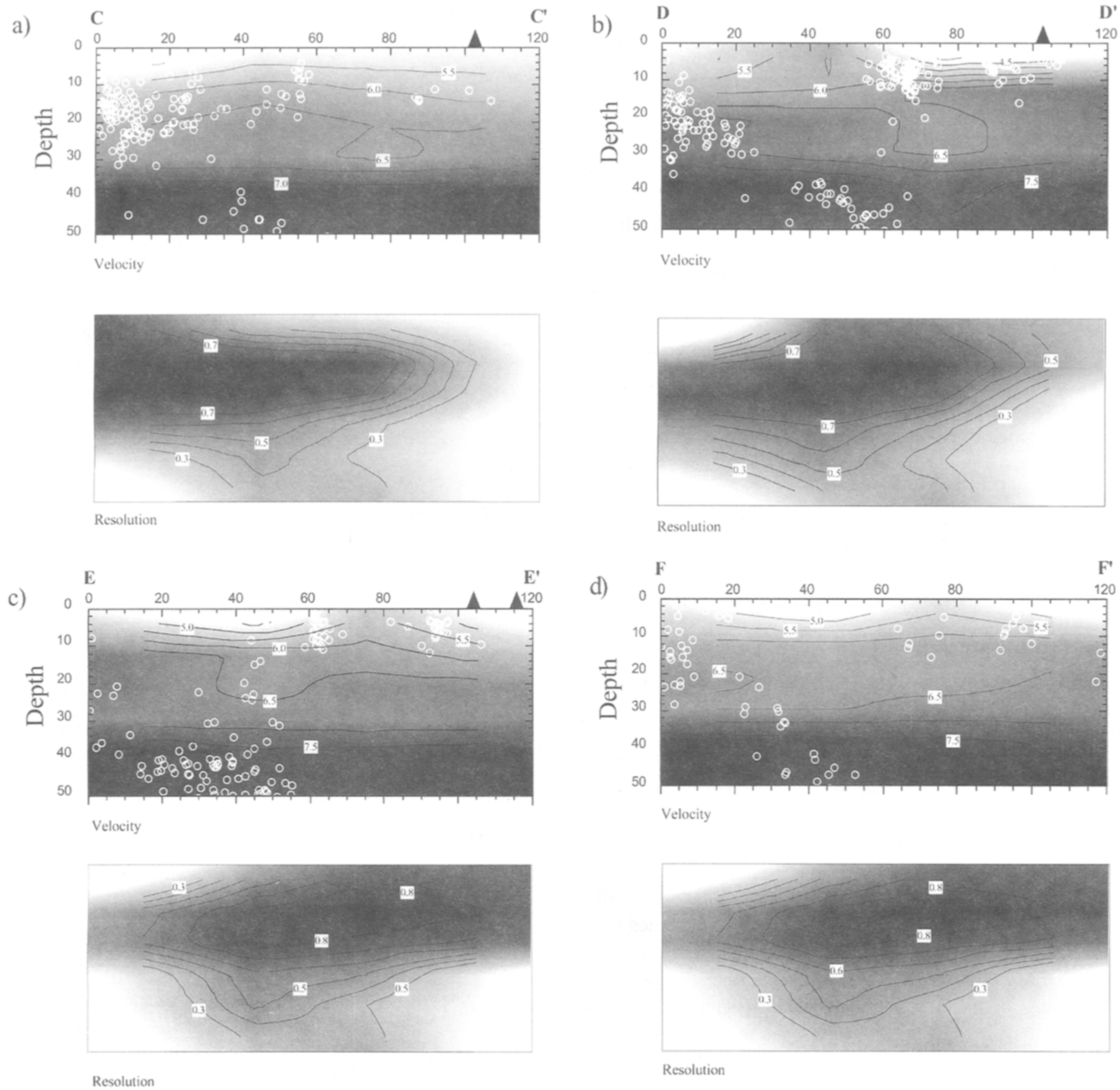

Figure 9. (a) through (d) Cross sections of *P*-wave velocities, relocated seismicity (white circles), and diagonal element resolution obtained from the coarse (40 × 40 × 10 km) grid. For location of cross sections, see Figures 3 and 7. Seismicity is projected from 20 km on each side of the cross-sectional lines.

anomaly in the NE central part of the inverted area (peaked at the intersection of lines D-D′ and K-K′, Fig. 7a) and two high-velocity anomalies SW and SE of the low-velocity anomaly (intersection of lines D-D′ with J-J′ and E-E′ with K-K′, respectively, Fig. 7a). The size and precise location of these velocity anomalies is influenced by the grid spacing even for the small-volume inversions (Fig. 8a). We believe that the low-velocity anomaly may be associated with elevated temperatures under the active volcanic chain. The fact that this low-velocity region is not centered beneath the volcanoes, but 20 km trenchward, may result from both our coarse grid spacing and low resolution toward the back-arc. The finer resolution results, using the small volume, show this low-velocity anomaly as an E–W elongated feature with its western portion offset trenchward from the volcanic chain but its eastern extension locating beneath the more southern volcanoes. The center of a Bouguer gravity low paralleling the southern portion of the volcanic chain is also offset toward the trench and is broad extending for more than 20 km on both sides of the axis of the volcanoes (Ponce and Case, 1987). The broad and offset gravity anomaly may indicate a wide region of elevated temperature beneath the volcanoes, which would be supported by our velocity results. Similar shallow low-velocity zones under active volcanoes have been found beneath Kilauea volcano in Hawaii (Thurber, 1984), beneath the volcanic arc in northern Honshu, Japan (Zhao *et al.,* 1992), and beneath the southern Cascades in northern California (Benz *et al.,* 1992). The low-velocity anomalies beneath Kilauea and the northern Honshu volcanic arc are nearly centered beneath the volcanoes, while similar to our observations in Costa Rica, the low velocities imaged beneath the southern Cascades are offset from the volcanic chain. The presently most active volcano (Kilauea) has low velocities centered directly beneath it, while the low velocities associated with the less-active volcanoes (southern Cascades and Costa Rica) are offset some 20 to 30 km from the volcanic edifices. Lack of resolution toward the NW prevents us from imaging this shallow low-velocity zone along the NW–SE continuation of the volcanic chain.

Since this low-velocity anomaly is coincident with outcrops of Quaternary volcanic rocks that extend southwest of the present volcanic chain (Fig. 2), an alternative interpretation of this anomaly is that it reflects surface geology rather than a subsurface feature. The magmatic history of Costa Rica indicates a progression from less silica-rich to more silica-rich products from early Tertiary through the Quaternary. The relatively silica-enriched Quaternary volcanics may have lower seismic velocities compared with the older less-siliceous surrounding Tertiary volcanic rocks, producing a low-velocity anomaly.

A second, less-resolved, low-velocity zone near the surface appears just north of Quepos (intersection of lines E-E′ and J-J′, Figs. 7a and 9c) and may be associated with a NW–SE trending, Late Cretaceous to Late Tertiary sedimentary basin south of the Herradura peninsula (Fig. 10). This sedimentary basin overlies ophiolitic units and is composed of over 5 km of marine sediments (Rivier, 1985; Ponce and Case, 1987), ranging from pelagic limestones and turbidites (the oldest) to shallow water sandstones and conglomerates (the youngest) (Ludington *et al.,* 1987).

The areas where high-velocity anomalies appear at shallow depth have better resolution and are elongated parallel to the Middle America Trench (Fig. 7a); there are two distinct velocity highs in the coarse grid results that merge into a continuous feature sub-parallel to the Middle America Trench in the fine grid results (Fig. 8a). The western high-velocity anomaly (at the intersection of line D-D′ with J-J′) correlates with surface exposures of ultramafic ophiolitic units of Jurassic to Early Tertiary age (Fig. 11). The eastern high-velocity anomaly is probably associated with the Talamanca batholith and with basic Tertiary volcanic units outcropping on the Talamanca Cordillera (Fig. 11). Velocities

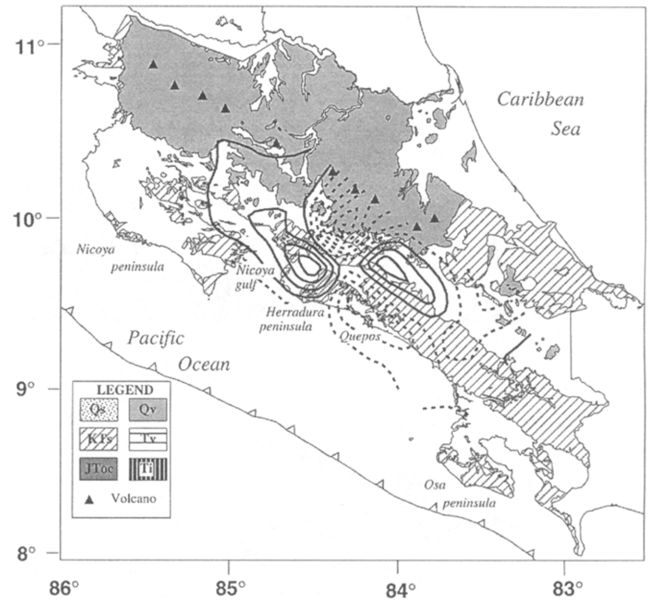

Figure 10. Correlation between shallow (less than 10 km) velocities obtained from the coarse grid inversions with sedimentary rocks (KTs) and with the active volcanic chain. Dashed contours represent velocities less than 5.0 km/sec and solid contours greater than 5.0 km/sec. Note the coincidence between the low velocities and the geologic units indicated.

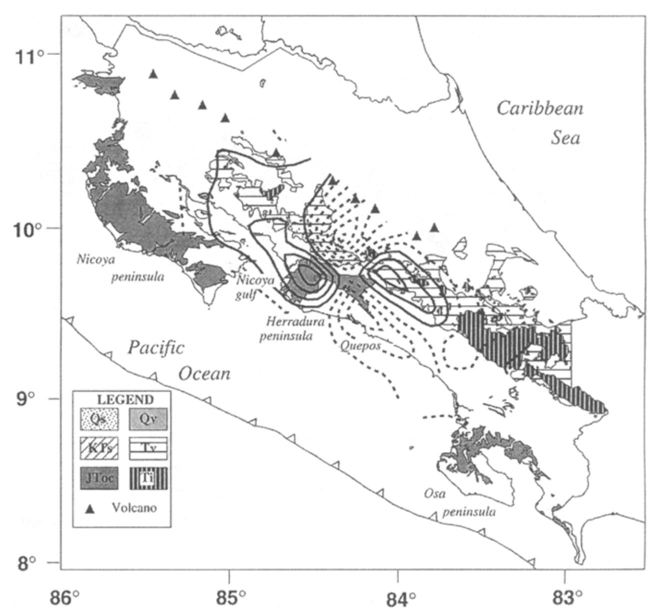

Figure 11. Correlation between shallow (less than 10 km) velocities obtained from the coarse grid inversions with ocean floor rocks (JToc), Tertiary intrusive (Ti), and volcanic (Tv) rocks. Contours are the same as in Figure 10. Note the coincidence between the high velocities (solid contours) and the geologic units indicated.

associated with the Talamanca plutonic rocks probably vary considerably since their silica content scatters widely between 46% and 72% (Williams and McBirney, 1969); however, regardless of specific rock type, their velocities should be faster than the surrounding sediments. Even though outcrops of the Tertiary intrusives are scarce in central Costa Rica, their presence indicates that the batholith extends this far north underlying the Tertiary volcanic units. These basic Tertiary volcanic units also outcrop trenchward from the active volcanic arc and might be responsible for the NW lobe of the western high.

The shallow low-velocity anomaly imaged near the active volcanoes does not extend to depth; at 10 km, it is replaced by higher velocities near D-D′ (Figs. 7b and 9b). Between depths of 20 and 30 km, a continuous ~80-km-long low-velocity anomaly parallel to the active volcanic chain is the most prominent feature in the velocity maps (Fig. 7d). This low-velocity region is substantially smaller and more circular in the images produced using station corrections. In central Costa Rica, this low-velocity anomaly is offset about 30 km trenchward from the active volcanoes; in the northernmost part of our study area, a smaller velocity low is offset 50 km trenchward from the active volcanoes. The large distance from the volcanoes argues against this anomaly resulting from elevated temperatures related to active magmatism. We interpret this anomaly to be a low-density intrusive remnant of an earlier phase of magmatic activity. From upper Cretaceous to the present, Costa Rica has been the site of continuous magmatic events, with the late Miocene being a particularly vigorous period generating the Talamanca intrusive series. The 20 km offset of the two low-velocity anomalies perpendicular to the Middle American Trench is nearly coincident with a tear (QSC in Fig. 1) in the subducting plate where the southeast section of the slab dips ~20° shallower than the northwestern section (Protti *et al.*, 1994). If the two low-velocity anomalies represent the same offset feature, the coincidence of that offset with a tear in the subducting plate suggests that its origin is tied to the subduction process. We do not image the low-velocity anomalies in the lower crust directly beneath the volcanoes as seen by Zhao *et al.* (1992) and Lees and Ukawa (1992) under the Japan arc, but we note that Zhao *et al.* (1992) also imaged low velocities in the lower crust offset up to 50 km trenchward from the volcanic chain.

High-velocity anomalies at lower crust–upper mantle depths, up to 5% higher than the average velocity for these depths, are found toward the trench (Figs. 7c, 7d, and 9), and we believe they are imaging the cooler oceanic Cocos plate as it plunges beneath Costa Rica. Lack of resolution is probably inhibiting our imaging of these high velocities to the SE. The fine grid inversions cannot image the slab because within this volume the slab is deeper than 30 km (Fig. 1), and we have poor resolution below this depth. At a 30-km depth, the high velocities that we interpret as the subducting Cocos plate are disrupted, toward the southeast, by a northeast–southwest elongate low-velocity region (Fig. 7d). The location and trend of this low-velocity anomaly correlates with the extension of the Cocos Ridge as it subducts beneath Costa Rica. The Cocos Ridge is a 200- to 300-km-wide shallow (about 2000-m shallower than the surrounding sea floor, Fig. 1) bathymetric feature resulting from passage of the Galapagos hot spot. Seismic refraction and gravity data indicate that a thickened oceanic crust of about 14 km (Bentley, 1974) is responsible for the high elevation of the Cocos Ridge. The low velocities we obtain near a depth of 30 km in the region of the subducted Cocos Ridge are most likely due to its thick crustal root compared with adjacent subducted oceanic lithosphere.

We find a good correlation between our shallow velocity model and the published Bouguer gravity map for Costa Rica (Ponce and Case, 1987) (Fig. 12). Low velocities seem to correlate with negative gravity anomalies, and high velocities, with positive gravity anomalies. The negative Bouguer anomalies are associated with both the active volcanic chain and sedimentary basins where we also find low seismic activity. The most conspicuous gravity anomaly in Costa Rica is a large NW-trending low extending from Panama to just south of the Herradura peninsula (Ponce and Case, 1987), where it correlates with shallow low velocities (Fig. 12). Lees and Ukawa (1992) found a correlation of a low-velocity anomaly with a low Bouguer anomaly near the Izu peninsula, Japan, and Thurber (1983) showed an association between near-surface high and low velocities with high- and low-gravity anomalies in the Coyote Lake region, California. The highest positive gravity anomalies are associated

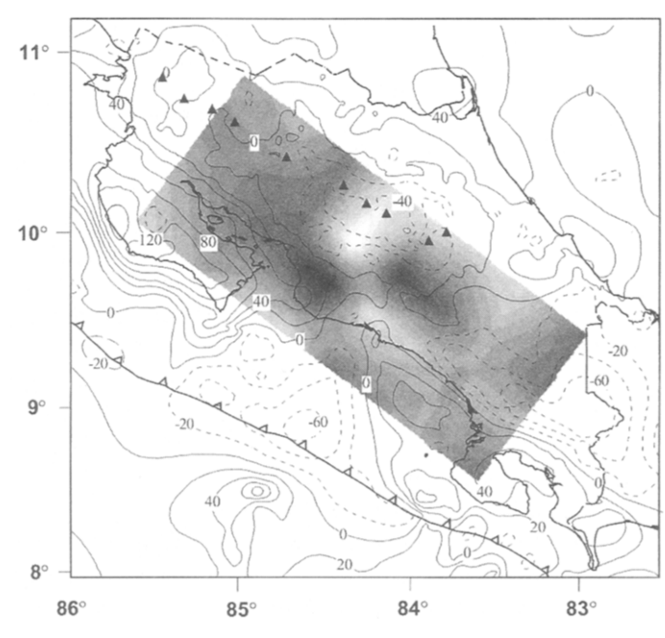

Figure 12. Correlation between shallow low (light pattern) and high (dark pattern) velocities obtained from the coarse grid inversions with Bouguer anomalies (contours in mGal) from Ponce and Case (1987).

with outcrops of the ophiolitic units in western Costa Rica. Other positive anomalies appear to follow surface outcrops of the Tertiary volcanic units or areas where these units approach the surface, such us near Limón, in the Caribbean (Protti and Schwartz, 1994). A ridge in the gravity anomalies connecting the Pacific with the Caribbean, across central Costa Rica, matches reasonably well our distribution of high velocities at shallow depths (Fig. 12).

Earthquake Locations

The earthquake locations obtained with the three-dimensional velocity structure have average residuals of 0.12 and 0.09 sec, for the coarse- and fine-grid inversions, respectively, 60% and 69% lower than locations using the starting one-dimensional velocity model. These new locations do not differ drastically from the initial locations; epicentral locations and focal depths differ, in a nonsystematic way, by an average of 3.3 and 5.0 km, respectively (3.1 and 4.4 km for the small-grid inversion). Since the events used in the inversions were selected from the best in the data base, the small changes in location indicate that (1) most of the information contained in the travel time residuals was put into the velocity structure, and (2) for events with good station coverage and relatively large numbers of arrival times, a simple one-dimensional structure can provide acceptable locations for routine earthquake location procedures. The three-dimensional velocity structure will be helpful in the location of events with either bad coverage or few arrival times or when more precise locations are desirable.

Figures 7 through 9 show the new earthquake locations superimposed on our three-dimensional velocity model both in map view as well as in cross sections perpendicular to the trench. There is a slight tendency for high seismicity to concentrate in areas of high velocity and to surround low-velocity regions; inside these low-velocity regions, seismic activity is relatively scarce. This is particularly evident for the shallow low-velocity anomalies near the active volcanoes (Figs. 7a and 9a), for the eastern shallow high-velocity anomaly (Fig. 7a), and for the high-velocity anomaly along the subducting slab (Fig. 9). The shallow seismicity pattern varies in depth following the 6.5 km/sec velocity contour (Fig. 9). A similar pattern was reported by Michael and Eberhart-Phillips (1991), who found that shallow seismicity in central California followed the 4.5 and 6.0 km/sec velocity contours, with little seismic activity within low-velocity sedimentary basins. This indicates a relationship between the seismogenic zone and rock type and rock properties. Thurber (1984) also found earthquakes clustering around a low-velocity zone directly beneath the Kilauea, Hawaii, caldera at shallow depths and an aseismic zone coinciding with the region of low velocities. Clustering of seismicity around the low-velocity region directly under the volcanoes may indicate deformation of the country rock by magma injection, while the scarce seismicity inside the low-velocity regions might be associated with the presence of partially molten rocks that impede brittle deformation. On the other hand, Zhao *et al.* (1992) found low-velocity anomalies in the crust associated with high seismicity that they interpreted as the seismicity producing a highly fractured medium that decreased the speed of seismic waves.

Earthquakes occurring in the deep high-velocity regions define a ~25-km-thick seismic slab. Our poor resolution at those depths inhibit accurate thickness estimates from our tomographic results.

Conclusions

Arrival time data from a regional short-period seismic network are used to resolve three-dimensional *P*-wave velocity variations beneath central Costa Rica. The resulting velocity model correlates well with local geology at shallow depth and with regional tectonic features at greater depth. We find low-velocity anomalies in the shallow crust near, but offset toward the trench from the active volcanoes, indicating either elevated temperatures in the subsurface or reflecting lower velocities of the Quaternary volcanics that outcrop at the surface or other units that directly underlie the volcanics. Shallow low velocities are also associated with a NW–SE trending Late Cretaceous to Late Tertiary sedimentary basin SE of Herradura Peninsula. Shallow high-velocity anomalies correlate with outcrops of ultramafic ophiolitic units, with the Talamanca batholith and with basic Tertiary volcanic units. Deeper high-velocity anomalies are associated with the subducting Cocos plate under Costa Rica and are disrupted by a northeast–southwest elongate low-velocity anomaly that correlates with subduction of the aseismic Cocos Ridge. We interpret a prominent low-velocity body between depths of 20 and 30 km as a low-density intrusive remnant of an earlier phase of magmatic activity.

The large variations in velocity that we image in the upper 10 km of the crust (over 20% perturbations) are probably concentrated at very shallow depths. These strong lateral velocity variations will have a dramatic effect on local and regional distance wave propagation. The model of the shallow structure that we obtained will therefore be important for improving the determination of Costa Rica earthquake source parameters from surface- and body-wave modeling. Improved source parameters are essential in helping to understand the tectonic processes responsible for generating large earthquakes on both coasts of Costa Rica.

Acknowledgments

This study was made possible through the hard work of the staff at the Costa Rica Volcanological and Seismological Observatory in the systematic collection and processing of seismic information to produce such a complete data base. We thank D. Eberhart-Phillips for providing the computer code used for the inversions, John Vidale and Chuck Ammon for their comments on an earlier version of this manuscript, and William Prothero, Jose Pujol, and Dean Whitman for their thorough reviews of the manuscript. Support for this research was provided by NSF Grant EAR-9018487 and by the U.S. Department of Energy, under Contract Number W-7405-ENG-48 to the Lawrence Livermore National Laboratory. OFDA-USAID Grants

PDC GSS221300 and ASB G00401500 funded the installation of the seismic network in Costa Rica. The W. M. Keck Foundation provided partial support for instrumentation and computer facilities. This is Contribution Number 246 of the W. M. Keck Seismological Laboratory and the Institute of Tectonics and Contribution Number 176 of the Observatorio Vulcanológico y Sismológico de Costa Rica.

References

Bentley, L. R. (1974). Crustal structure of the Carnegie Ridge, Panama Basin, and Cocos Ridge, *Master's Thesis,* University of Hawaii, Honolulu, Hawaii, 49 pp.

Benz, H. J., G. Zandt, and D. H. Oppenheimer (1992). Lithospheric structure of northern California from teleseismic images of the upper mantle, *J. Geophys. Res.* **97,** 4791–4807.

DeMets, C., R. G. Gordon, D. F. Argus, and S. Stein (1990). Current plate motions, *Geophys. J. Int.* **101,** 425–478.

Eberhart-Phillips, D. (1986). Three-dimensional velocity structure in the northern California coast ranges from inversion of local earthquake arrival times, *Bull. Seism. Soc. Am.* **76,** 1025–1052.

Eberhart-Phillips, D. (1990). Three-dimensional P and S velocity structure in the Coalinga region, California, *J. Geophys. Res.* **95,** 15343–15363.

Fan, G. W., S. L. Beck, and T. C. Wallace (1993). The seismic source parameters of the 1991 Costa Rica aftershock sequence: evidence for a transcurrent plate boundary, *J. Geophys. Res.* **98,** 15759–15778.

Fisher, D. M., T. W. Gardner, J. S. Marshall, and W. Montero (1994). Kinematics associated with late Cenozoic deformation in central Costa Rica: western boundary of the Panama microplate, *Geology* **22,** 263–266.

Goes, S. D. B., A. A. Velasco, S. Schwartz, and T. Lay (1993). The April 22, 1991, Valle de la Estrella, Costa Rica (Mw = 7.7) earthquake and its tectonic implications: a broadband seismic study, *J. Geophys. Res.* **98,** 8127–8142.

Güendel, F., K. C. McNally, J. Lower, M. Protti, R. Sáenz, E. Malavassi, J. Barquero, R. Van Der Laat, V. González, C. Montero, E. Fernández, D. Rojas, J. Segura, A. Mata, and Y. Solís (1989). First results from a new seismographic network in Costa Rica, Central America, *Bull. Seism. Soc. Am.* **79,** 205–210.

Güendel, F. and J. Pacheco (1992). The 1990–1991 seismic sequence across central Costa Rica: evidence for the existence of a micro-plate boundary connecting the Panama deformed belt and the Middle America trench, *EOS* **73,** 399.

Jacob, K. H. and J. Pacheco (1991). The M-7.4 Costa Rica earthquake of April 22, 1991: tectonic setting, teleseismic data, and consequences for seismic hazard assessment, *Earthquake Spectra* **7,** Suppl. B.

Klein, F. W. (1978). Hypocenter location program Hypoinverse, *U.S. Geol. Surv. Open-File Rept. 78-694,* 113 pp.

Lees, J. M. and M. Ukawa (1992). The south Fossa Magna, Japan, revealed by high-resolution P- and S-wave travel time tomography, *Tectonophys* **208,** 377–396.

Liaw, H. B. (1981). Seismic velocity modeling from an ensemble of earthquakes, *Ph.D. Thesis,* University of Texas, Dallas, 135 pp.

Ludington, S., R. Castillo, and H. Azuola (1987). Geology of Costa Rica, in mineral resources assessment of the Republic of Costa Rica, *U.S. Geol. Surv. Misc. Invest. Map I-1865,* 6–7.

Matumoto, T., M. Othake, G. Latham, and J. Umaña (1977). Crustal structure of southern Central America, *Bull. Seism. Soc. Am.* **67,** 121–134.

Michael, A. and D. Eberhart-Phillips (1991). Relations among fault behavior, subsurface geology, and three-dimensional velocity models, *Science* **253,** 651–654.

O'Connell, D. R. H. and L. R. Johnson (1991). Progressive inversion for hypocenters and P wave and S wave velocity structure: Application to the Geysers, California, geothermal field, *J. Geophys. Res.* **96,** 6223–6236.

Pavlis, G. L. and J. R. Booker (1980). The mixed discrete-continuous inverse problem: application to the simultaneous determination of earthquake hypocenters and velocity structure, *J. Geophys. Res.* **85,** 4801–4810.

Ponce, D. A. and J. E. Case (1987). Geophysical interpretation of Costa Rica, in Mineral resources assessment of the Republic of Costa Rica, *U.S. Geol. Surv. Misc. Invest. Folio, I-1865,* 8–17.

Protti, M. and S. Schwartz (1994). Mechanics of back-arc deformation in Costa Rica: evidences from an aftershock study of the April 22, 1992 Valle de la Estrella earthquake (Mw = 7.7), *Tectonics* **13,** 1093–1107.

Protti, M., K. McNally, and F. Güendel (1994). The geometry of the Wadati-Benioff zone under southern Central America and its tectonic significance: results from a high-resolution local seismographic network, *Phys. Earth. Planet. Interiors* **84,** 271–287.

Rivier, S. F. (1985). Sección geológica del Pacífico al Atlántico a través de Costa Rica, *Rev. Geol. Am. Central* **2,** 23–32.

Silver, E. A., D. L. Reed, J. E. Tagudin, and D. J. Heil (1990). Implications of the north and south Panama thrust belt for the origin of the Panama orocline, *Tectonics* **9,** 261–281.

Thurber, C. H. (1983). Earthquake locations and three-dimensional crustal structure in the Coyote lake area, central California, *J. Geophys. Res.* **88,** 8226–8236.

Thurber, C. H. (1984). Seismic detection of the summit magma complex of Kilauea Volcano, Hawaii, *Science* **223,** 165–167.

Thurber, C. H. (1992). Hypocenter-velocity structure coupling in local earthquake tomography, *Phys. Earth. Planet Interiors* **75,** 55–62.

Um, J. and C. Thurber (1987). A fast algorithm for two-point seismic ray-tracing, *Bull. Seism. Soc. Am.* **77,** 972–986.

Verdonck, D. and G. Zandt (1994). Three-dimensional geometry of the Mendocino triple junction, *J. Geophys. Res.* **99,** 23843–23858.

Williams, H. and A. R. McBirney (1969). Volcanic history of Honduras, *Univ. Calif. Publ. Geol. Sci.* **85,** 1–101, Berkeley and Los Angeles.

Zhao, D., A. Hasegawa, and S. Horiuchi (1992). Tomographic imaging of P and S wave velocity structure beneath northeastern Japan, *J. Geophys. Res.* **97,** 19909–19928.

Observatorio Vulcanológica y Sismológico de Costa Rica
Universidad Nacional, Apdo. 86-3000
Heredia, Costa Rica
(M.P.)

Earth Sciences Department and Institute of Tectonics
University of California
Santa Cruz, California 95064
(S.Y.S.)

Institute of Geophysics and Planetary Physics
Lawrence Livermore National Laboratory
Livermore, California 94550
(G.Z.)

Manuscript received 2 September 1994.